Virus Evolution, 2024, **10(1)**, veae084
DOI: https://doi.org/10.1093/ve/veae084
Advance Access Publication 3 October 2024
Research Article

Influenza A virus within-host evolution and positive selection in a densely sampled household cohort over three seasons

Emily E. Bendall[1], Yuwei Zhu[2], William J. Fitzsimmons[3], Melissa Rolfes[4], Alexandra Mellis[4], Natasha Halasa[5], Emily T. Martin[6], Carlos G. Grijalva[7], H. Keipp Talbot[7,8], Adam S. Lauring[1,3,*]

[1]Department of Microbiology & Immunology, University of Michigan, Ann Arbor, MI 48109, United States
[2]Department of Biostatistics, Vanderbilt University Medical Center, Nashville, TN 37203, United States
[3]Division of Infectious Diseases, University of Michigan, Ann Arbor, MI 48109, United States
[4]Influenza Division, Centers for Disease Control and Prevention, Atlanta, GA 30333, United States
[5]Department of Pediatrics, Vanderbilt University Medical Center, Nashville, TN 37203, United States
[6]Department of Epidemiology, University of Michigan, Ann Arbor, MI 48109, United States
[7]Department of Health Policy, Vanderbilt University Medical Center, Nashville, TN 37203, United States
[8]Department of Medicine, Vanderbilt University Medical Center, Nashville, TN 37203, United States

*Corresponding author. Division of Infectious Diseases, University of Michigan, 1137 Catherine St., MS2 Room 4742C, Ann Arbor, MI 48109, United States.
E-mail: alauring@med.umich.edu

Abstract

While influenza A virus (IAV) antigenic drift has been documented globally, in experimental animal infections, and in immunocompromised hosts, positive selection has generally not been detected in acute infections. This is likely due to challenges in distinguishing selected rare mutations from sequencing error, a reliance on cross-sectional sampling, and/or the lack of formal tests of selection for individual sites. Here, we sequenced IAV populations from 346 serial, daily nasal swabs from 143 individuals collected over three influenza seasons in a household cohort. Viruses were sequenced in duplicate, and intrahost single nucleotide variants (iSNVs) were identified at a 0.5% frequency threshold. Within-host populations exhibited low diversity, with >75% mutations present at <2% frequency. Children (0–5 years) had marginally higher within-host evolutionary rates than adolescents (6–18 years) and adults (>18 years, 4.4×10^{-6} vs. 9.42×10^{-7} and 3.45×10^{-6}, $P < .001$). Forty-five iSNVs had evidence of parallel evolution but were not over-represented in HA and NA. Several increased from minority to consensus level, with strong linkage among iSNVs across segments. A Wright–Fisher approximate Bayesian computational model identified positive selection at 23/256 loci (9%) in A(H3N2) specimens and 19/176 loci (11%) in A(H1N1)pdm09 specimens, and these were infrequently found in circulation. Overall, we found that within-host IAV populations were subject to genetic drift and purifying selection, with only subtle differences across seasons, subtypes, and age strata. Positive selection was rare and inconsistently detected.

Keywords: influenza virus; evolution; mutation; genetic drift; natural selection; household

Introduction

Seasonal influenza A virus (IAV) evolution is dominated by antigenic drift. As the population gains immunity to circulating strain(s), antigenically distinct strains continue to emerge, displacing previous strains and forcing a change in the annual vaccine strain (Smith et al. 2004, Bedford et al. 2015). Accordingly, understanding the drivers of recurrent positive selection of antigenic variants is important for vaccine strain selection (Salk and Suriano 1949, Kilbourne et al. 2002, De et al. 2013). All genetic variation that is present in the virus population, including new antigenic variants, is ultimately derived from mutations that arise within individual hosts. Within host processes may at times parallel those seen at a global scale, as partial immunity from vaccination or previous infections may act as a selective force promoting the evolution of new antigenically distinct variants (Volkov et al. 2010, Luo et al. 2012).

As with many acute viral infections, the within-host dynamics of influenza virus are dominated by genetic drift and characterized by low levels of genetic diversity (Dinis et al. 2016, Sobel Leonard et al. 2016, Debbink et al. 2017, McCrone et al. 2018, Koel et al. 2020, Xue and Bloom 2020, Han et al. 2021). However, there is mixed evidence for specific sites being under positive selection.

Several studies have reported nonsynonymous mutations in antigenic sites (Dinis et al. 2016, Debbink et al. 2017, McCrone et al. 2018, Koel et al. 2020, Han et al. 2021), and these sites are occasionally shared among individuals (Dinis et al. 2016, Debbink et al. 2017), exist at high frequency (Dinis et al. 2016, Koel et al. 2020, Han et al. 2021), or are found at detectable levels in the global population (McCrone et al. 2018, Koel et al. 2020). More often, these mutations are identified only in single individuals at low (<5%) frequencies. Additionally, the frequency and number of mutations tend not to differ between antigenic and nonantigenic sites (McCrone et al. 2018, Xue and Bloom 2020).

Within-host selection may not be uniform across host populations. While we have found that vaccination has minimal impact on patterns of within-host diversity, other factors, such as age, have not been thoroughly explored (Debbink et al. 2017). Children have prolonged shedding compared to adults, and the extra time may allow for mutations in antigenic sites and their subsequent selection (Ng et al. 2016). A recent study focused on young children (<5 years old), took place in Southeast Asia where child vaccination rates are very low, and most children did not have detectable antibody titers in the study (Han et al. 2021). Mutations were identified in antigenic sites, but there was not a clear signal of positive selection. By contrast, most adolescents (e.g. ages 6–17 years) will have had multiple exposures to influenza (Bodewes et al. 2011), with a shedding period that is of intermediate length (Ng et al. 2016). This combination may be optimal for the selection of new antigenic variants within hosts, but there have not been any studies focused on this group.

There are several technical reasons why positive selection has been difficult to detect. Selection is difficult to detect and quantify with cross-sectional sampling, and most studies have reported one or two samples per subject without longitudinal sampling (Koel et al. 2020). Second, the frequency threshold for detecting intrahost single nucleotide variants (iSNVs) is typically 2%. Most intrahost variants are *de novo* mutations due to tight bottlenecks during transmission and the detection threshold may be too high to detect many of these iSNVs (Sobel Leonard et al. 2016, 2017b, McCrone et al. 2018). Finally, there are few formal tests for positive selection on a per-site basis; most interrogate on a gene level (e.g. nucleotide diversity), or informally on a per-site basis (e.g. iSNVs at important sites). In some cases, single mutations are sufficient to cause antigenic drift making per-site tests necessary to detect selection for antibody escape (Doud et al. 2017).

Here, we address the design and technical limitations of previous studies. We developed and benchmarked a sequencing and bioinformatics pipeline that allowed us to accurately identify iSNVs at a frequency threshold of 0.005 (0.5%). We applied this method to individuals sampled within a case-ascertained household cohort, in which nasal swab specimens were collected every day for 7 days after symptom onset. The study covered three influenza seasons and included individuals across the age spectrum with a mixture of antiviral treatment and vaccination histories. We use these sequences and host data to define patterns of within-host genetic diversity and divergence with respect to age, vaccination, antiviral usage, and timing of sample collection. We applied multiple methods to detect selection on a per-site basis with clear statistical cutoffs.

Materials and methods

Cohort and specimens

Households were enrolled through the Influenza Transmission Evaluation Study (FluTES), a case-ascertained household transmission study based in Nashville, TN, that enrolled over the 2017/18, 2018/19, and 2019/20 Northern Hemisphere influenza seasons (Rolfes et al. 2023). All individuals provided informed consent, and the study was approved by the Vanderbilt University Medical Center Institutional Review Board. The first household members with laboratory-confirmed IAV infection (index cases, always symptomatic) were identified and recruited from ambulatory clinics, emergency departments, or other settings that performed influenza testing. For this study, we focused on IAV only. Index cases with acute illness of <5-day duration who lived with at least one other person who was not currently ill were eligible to participate. The index case and their household contacts were enrolled within 7 days of the index case's illness onset. Influenza vaccination was self-reported at enrollment and was included if both date and location of vaccination were provided. Participants (index cases and household contacts) who reported vaccination within 14 days prior to illness onset in the household had their vaccine status listed as unknown. For individuals with an asymptomatic infection, the symptom onset date of the index case was used as that individual's onset date. Individuals were divided into three age groups: children (≤5 years), adolescents (6–17 years), and adults (≥18 years) for further analyses.

Nasal swabs were self-/parent-collected daily during follow-up for 7 days and tested for influenza using reverse transcription quantitative polymerase chain reaction (RT-qPCR) at the Vanderbilt University Medical Center using the Centers for Disease Control and Prevention (CDC) Human Influenza Virus Real-Time RT-PCR Diagnostic Panel, Influenza A/B Typing Kit with the SuperScript III Platinum One-Step qRT-PCR Kit (Invitrogen) on the StepOnePlus or QuantStudio 6 Flex (Applied Biosystems). Subtyping of IAV-positive specimens was performed using the CDC Human Influenza Virus Real-Time RT-PCR Diagnostic Panel, Influenza A Subtyping Kit with the SuperScript III Platinum One-Step qRT-PCR Kit System on the MagNA Pure LC 2.0 platform (Roche).

Benchmarking variant calling

We used data from McCrone et al. (2016) to benchmark our variant calling pipeline. Briefly, 20 viruses, each with a single point mutation, were generated in a WSN33 background. The 20 mutant viruses were mixed with wild-type WSN33 to create populations in which each mutant was present at 5%, 2%, 1%, and 0.5%. These samples were processed and sequenced in duplicate on an Illumina MiSeq. We aligned the data to WSN33 using Bowtie2 (Langmead and Salzberg 2012) with the "very sensitive" setting, and duplicate reads were discarded using Picard tools (Picard Toolkit 2019). Reads from both replicates of a given specimen were combined and used to make a within-host consensus sequence using a script from Xue and Bloom 2020). The replicates were then separately aligned to this consensus, and duplicates were removed. iSNVs were called using iVAR in each replicate (Grubaugh et al. 2019). To be considered for variant calling, reads had to have a mapping quality of ≥20, and bases had to have a phred score of ≥30. iSNVs had to have a per-site sequencing depth of ≥400, and an iVAR *P*-value of $\leq 1 \times 10^{-5}$. iSNVs were retained only if they were called in both sequencing replicates. We calculated the specificity and sensitivity for iSNV detection at each frequency threshold (0.5%, 1%, 2%, and 5%).

Sequencing

IAV-positive samples with an RT-qPCR cycle threshold (C_t) value of ≤30 were sequenced in duplicate after the ribonucleic acid (RNA) extraction step. RNA was extracted using Invitrogen PureLink Pro 96 Viral RNA/DNA Purification Kits on an EpiMotion or a MagMAX

viral/pathogen nucleic acid purification kit (ThermoFisher) on a Kingfisher Machine. SuperScript IV one-step RT-PCR kits and universal IAV primers were used for RT-PCR (Hoffmann et al. 2001). Library preparation was completed by using the Illumina DNA Prep Kit, and libraries were sequenced on a Novaseq (2 × 150 PE reads) by the Advanced Genomics Core at the University of Michigan.

Reads from each sample were aligned to the vaccine strain for each subtype and year for the initial alignment: A/Michigan/45/2015 (H1N1)pdm09, A/Hong Kong/4801/2014 (H3N2), and A/Singapore/INFIMH-16-0019/2016. For 2019/20 A(H1N1)pdm09, we used A/New Jersey/13/2018 (EPI_ISL_319740), since the A/Brisbane/02/2018 sequence was not available. Variant calling was performed as mentioned earlier on samples in which each replicate had an average genome-wide coverage of at least 1000× (post de-duplication) and an iSNV frequency of ≥0.005 (0.5%). For iSNV in overlapping open reading frames (ORF), an iSNV was classified as a nonsynonymous if it was nonsynonymous in any ORF. Stop codons were classified as nonsynonymous. An iSNV's classification was consistent across all samples. For all further analyses, we used the average iSNV frequency in the two replicates as the iSNV frequency.

iSNV dynamics and divergence rates

We calculated the divergence rate using the methods from Xue and Bloom (2020). Briefly, we calculated the rate of evolution by summing the frequencies of within-host mutations (relative to the first sample consensus sequence or "founder" of the population) and divided by the number of available sites and time since the infection began. To account for iSNVs that go from minor to major allele in individuals with multiple samples, the allele frequency used was from the minor allele in the earliest sample. We calculated the rates separately for nonsynonymous and synonymous mutations. We used 0.75 for the proportion of available sites for nonsynonymous mutations and 0.25 for synonymous. To determine the number of available sites, we multiplied the proportion of sites available by the length of the coding sequence for the relevant reference. We excluded M and NS segments, because overlapping open reading frames allow an individual mutation to be both synonymous and nonsynonymous. Because symptoms typically start 2–3 days postinfection, we added 2 days to the time since symptom onset to get the time since infection began (Baccam et al. 2006, Carrat et al. 2008, Beauchemin and Handel 2011). We excluded individuals who were asymptomatic from the divergence rate analysis. We also excluded outlier samples that had ≥50 iSNVs.

We calculated the rate of evolution for each sample with nonsynonymous and synonymous rates calculated separately. Because the calculated rate of divergence varied over the course of the infection, we also calculated the rate using the sample with the lowest C_t value for each individual. The rate was calculated for the whole genome and for each segment.

Analysis of shared iSNVs

We performed permutation simulations for each reference strain to determine the expected number of individuals who would share an iSNV based on the number of individuals, the number of iSNVs, and the genome size (Valesano et al. 2020). We set the proportion of the genome that was mutable as 0.6 based on experimental data (Visher et al. 2016). One thousand permutations were performed for each reference strain. For a given group (e.g. mutations shared between two individuals), we calculated the *P*-value as the proportion of permutations that had as many or more shared iSNVs than the observed number of shared iSNVs. Because we were interested in the number of times that an iSNV independently arose, iSNVs that were shared among multiple individuals within the same household were recorded only once for that household for both the simulations and the observed number of individuals. Samples and individuals with >50 iSNVs were excluded.

Wright Fisher approximate Bayesian computational method

We mapped the allele trajectory of alleles that changed from a minor to a major allele over the course of an infection. We also used a Wright Fisher approximate Bayesian computational (WFABC) method to estimate the effective population size (Ne) and per locus selection coefficient (s) based on allele trajectories (Foll et al. 2015). A generation time of 6 h was used (Baccam et al. 2006). To maximize the number of loci used in the calculation of Ne and to avoid violating the assumption that most loci are neutral, we estimated a single Ne for A(H1N1)pdm09 and for A(H3N2). We used all loci in which the first two time points were 1 day apart to estimate Ne. Ten thousand bootstrap replicates were performed.

A fixed Ne was used for the per locus selection coefficient simulations, with the analysis repeated for the mean Ne, and ± 1 SD estimated from the previous step. A uniform prior between *s* of −0.5 and 0.5 was used. One hundred thousand simulations with an acceptance rate of 0.01 were used. We estimated the 95% highest posterior density intervals using the boa package (Smith 2007) in R. We considered a site to be positively selected if the 95% highest posterior density did not include 0 for all three effective population sizes. For both sets of analyses, iSNV frequency was in relation an individual's first sequenced sample.

Statistical methods

Descriptive statistics were conducted. The Mann–Whitney *U* tests were used to compare the number of iSNVs per sample and iSNV frequencies by mutation type, vaccination, and antiviral usage. The Kruskal–Wallace tests were performed for age and days post-symptom onset. For divergence rates, Mann–Whitney *U* tests were performed for vaccination, antiviral usage, and IAV subtype. Kruskal–Wallace tests were performed for age, segment, and days postinfection. We also compared the likelihood of a shared iSNV or a positive selection coefficient. χ^2 tests were performed to test if age, vaccination, and antiviral usage affected the likelihood of an individual having a shared iSNV or impacted the probability of an individual having at least 1 iSNV with a positive selection coefficient. All analyses were conducted using R version v4.2.0.

Results

Benchmarking

The FluTES study was a case-ascertained household cohort that enrolled over the 2017/18 through 2019/20 Northern Hemisphere influenza seasons. Consistent with the viruses circulating in the USA during this timeframe, the 2017/18 (Garten et al. 2018) and 2018/19 (Xu et al. 2019) seasons were A(H3N2) predominant, and the 2019/20 flu season was exclusively A(H1N1)pdm09 (Dawood et al. 2020). In total, there were 302 cases at the Vanderbilt site over these three seasons, and the majority provided seven daily specimens. We successfully sequenced 346/413 (84%) specimens from 143 individuals (Table 1). Out of 143 (58%) individuals, 83 had multiple sequenced specimens (Supplementary Fig. S1). Among the 143 individuals, there were 37 children (≤5 years), 51 adolescents (6–17 years), and 55 adults (≥18 years).

Table 1. Overview of specimen types.

Subtype	Season	Number of specimens	Number of individuals
H3N2	2017–18	32	13
	2018–19	153	58
	2019–20	0	0
H1N1	2017–18	13	7
	2018–19	35	14
	2019–20	113	51

Table 2. Benchmarking results based on detection of 20 single nucleotide variants.

% Frequency	True positives	Sensitivity	False positives	Specificity
5	18	0.9	13	0.9996759
2	15	0.75	6	0.9998504
1	13	0.65	10	0.9997507
0.5	6	0.3	2	0.9999501

In order to accurately detect ultra-rare mutations, we refined our variant calling approach and benchmarked this new method against a previously described dataset (McCrone et al. 2016). In our benchmarking, we found high specificity across all mutant frequencies, but sensitivity decreased as mutant frequency decreased (Table 2). To detect the greatest number of true variants, we used a 0.005 frequency threshold for the rest of the study. We sequenced each specimen in duplicate, obtaining high coverage across the genome (mean >10 000×) and consistency in iSNV frequency between the sequencing replicates (Fig. 1a and b). iSNVs were more common in the third codon position compared to the first and second position at cutoff frequencies of >0.5%. As sequencing errors are presumably randomly dispersed, this further suggests that we are detecting true iSNVs (Fig. 1c).

Cross-sectional analysis

Most specimens had between 1 and 50 iSNVs at >0.5% frequency, while four specimens had 0 iSNV and five specimens had >50 iSNVs (Fig. 2a, Supplementary Table S1). Children had more iSNVs per specimen (median 11) than adolescents (median 7, $P = .001$, Supplementary Fig. S2). The number of iSNVs per specimen increased as the infection progressed before decreasing again, mirroring typical viral titer trajectories (Supplementary Fig. S2). However, the difference in the number of iSNVs was not significant. The number of iSNVs did not vary much by vaccine status or antiviral usage (Supplementary Fig. S2). When corrected for available sites, the proportion of nonsynonymous iSNVs was much lower than that of synonymous (0.27 vs. 0.73).

The vast majority of iSNVs tended to be very low frequency and most were between 0.5% and 2% (Fig. 2b). The frequency of iSNVs varied significantly by day of sampling postsymptom onset ($P < .001$), host age ($P < .001$), mutation type ($P = .005$), vaccine status ($P < .001$), and antiviral usage ($P = .013$, Supplementary Table S1, Supplementary Fig. S3). Adults had the lowest median frequency (0.013), followed by children (0.014) and adolescents (0.015, Supplementary Fig. S3). Nonsynonymous iSNVs (median 0.015) were found at slightly higher frequencies than synonymous (median 0.013, Supplementary Fig. S3). Specimens from vaccinated individuals (median 0.015) had higher median iSNV frequencies than those from unvaccinated individuals (median 0.013, Supplementary Fig. S3c), while specimens from those receiving antivirals had lower iSNV frequencies (median 0.013 vs. 0.014, Supplementary Fig. S3b). While all of these differences were statistically significant, the magnitude of the differences was extremely small, and the iSNV frequency distributions almost completely overlapped.

We estimated within-host evolutionary rates as nucleotide divergence per site per day (Xue and Bloom 2020). Consistent with the expansion and contraction of the viral population over the course of an infection, the estimated divergence rate varied according to the day of sampling (Fig. 2, Supplementary Table S2). The measured divergence rate was the highest at ∼5–6 days postinfection and was lower when measured after that. This time-varying pattern was more pronounced for synonymous than nonsynonymous mutations. Children (0–5 years) had marginally higher within-host evolutionary rates than adolescents (6–18 years) and adults (>18 years, 4.4×10^{-6} vs. 9.42×10^{-7} and 3.45×10^{-6}, $P < .001$). (Supplementary Fig. S4). A(H1N1)pdm09 infections had a faster divergence rate than A(H3N2) for nonsynonymous mutations ($P = .010$, Fig. 2). The divergence rate did not vary by genome segment (Fig. 2), host antiviral usage, or host vaccination status (Supplementary Table S2).

Shared iSNV and evolutionary convergence

Evolutionary convergence can be a signal of positive selection and can be identified based on the sharing of iSNVs among individuals who are not linked by transmission. In our analysis, we first determined the expected number of iSNVs that would be shared based on chance alone given the number of sequenced specimens and iSNVs for each subtype and season. The corresponding threshold for statistical significance was ≥2 shared iSNVs for 2017/18 A(H3N2) and 2017/18 A(H1N1)pdm09, ≥4 for 2019/20 A(H1N1)pdm09, and ≥3 for 2018/19 A(H3N2) ($P < .001$ for all reference strains, Supplementary Fig. S5). Nearly all shared iSNVs were found at very low frequencies (Supplementary Fig. S6).

The hemagglutinin (HA) and neuraminidase (NA) genes did not exhibit an overabundance of shared iSNVs, and the frequencies of shared iSNVs in HA and NA were not higher than those of iSNVs in other genes. Only one shared iSNV was within an antigenic site, and it was synonymous (T620C [G197]). There was an overrepresentation of shared iSNVs in 2017/18 A(H3N2) M and NS with 28% and 45% of shared iSNVs despite these segments making up 8% and 6% of the genome, respectively. There was also an overrepresentation in 2017/18 and 2018/19 A(H1N1)pdm09 PB1 and M. They have 37% and 26% of the iSNV, but only make up 17% and 8% of the genome, respectively.

High iSNV specimens (>50 iSNVs) were responsible for 156/201 (78%) of shared iSNVs. Because these very high numbers of iSNVs are inconsistent with the typical rate of mutation accumulation and are plausibly due to low-level (<1%) contamination or coinfection, we repeated this analysis after removing specimens with >50 iSNVs. There was no effect on the number of shared iSNVs in HA and NA (Fig. 3). The number of iSNVs in 2017/18 and 2018/19 A(H1N1)pdm09 PB1, M, and 2017 A(H3N2) M segments were greatly decreased, but the over-representation of shared iSNVs in the 2017 A(H3N2) NS segment remained. When we plotted shared iSNVs in NS by individual, we found that most of the shared iSNVs were part of a low frequency, ∼400-bp haplotype shared among nine individuals (Supplementary Fig. S6).

Vaccination and antiviral usage did not affect the likelihood of an individual contributing to a shared variant (Supplementary Table S3). Host age did affect the likelihood, but no pairwise comparisons achieved statistical significance; 17% of iSNVs in adults were shared, 14% in adolescents, and 12% in children.

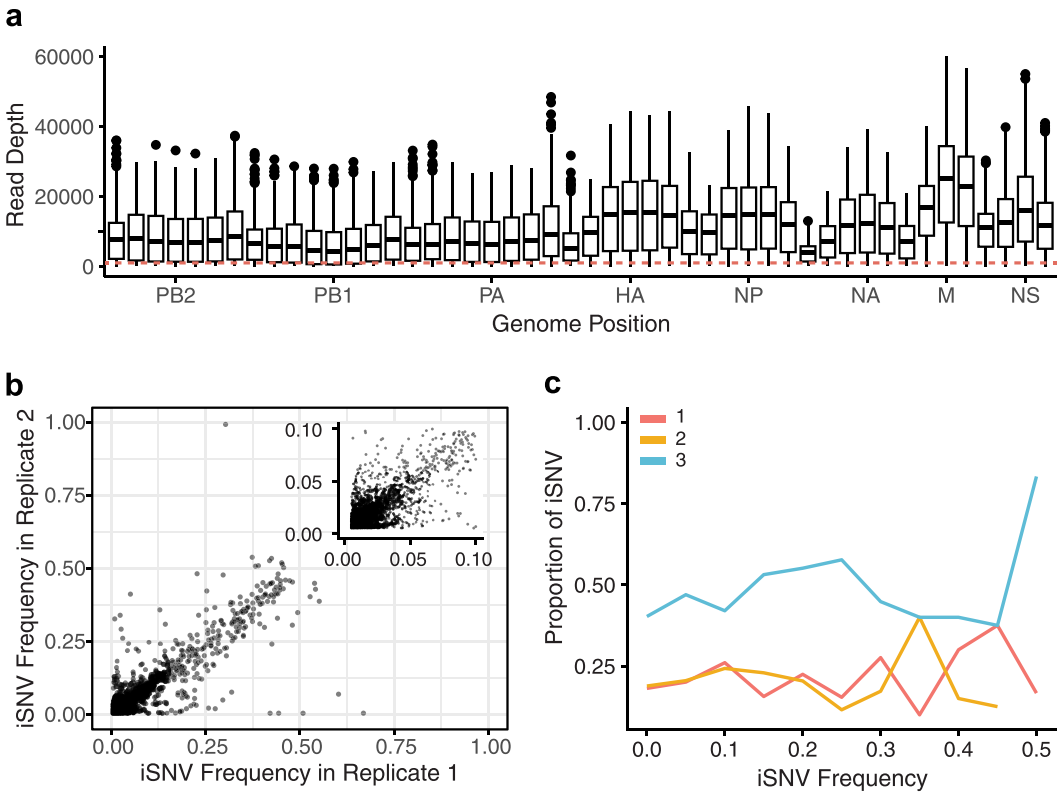

Figure 1. (a) Sequencing coverage across the genome in 300-bp nonoverlapping windows. The red dashed line denotes 1000×. The box shows the first quartile, median, and third quartile. The whiskers are 1.5× interquartile range. (b) iSNV frequency is consistent across replicates for iSNV present in both replicates. The insert shows iSNV frequency up to 0.1. The Pearson correlation coefficients are 0.55 and 0.89 for iSNVs at 0.5–5% and >5%, respectively. (c) Proportion of iSNVs in each codon position for a given frequency in 0.05 frequency bins. iSNVs in Codon Position 3 (blue) are more common than iSNVs in Position 1 (red) or 2 (gold) across the frequency range.

Analysis of selection in serial specimens

Thirty iSNVs changed from a minor to a major allele during an infection. This included two synonymous (G665A [A212] and G686A [T219]) and two nonsynonymous iSNVs (C556A [T176K] and G564A [A179T]) in HA antigenic sites from A(H3N2) infections. Importantly, there was evidence for linkage disequilibrium and hitchhiking, with neutral synonymous iSNVs being swept along with putatively selected nonsynonymous iSNVs (Sobel Leonard et al. 2017a). Eight individuals had >1 iSNVs that became the major allele, and in many cases, the allele trajectories of these iSNVs closely matched each other, even when present on different segments (Fig. 4a). For example, individual 1 811 602 (H3N2) had iSNVs at three loci on HA, NP, and PB2 (♦ in Fig. 4a) with very similar trajectories. The iSNVs on HA and NP are nonsynonymous, while the iSNV on PB2 is synonymous.

We used a WFABC method to infer selection coefficients on individual iSNVs. For A(H1N1)pdm09 and H3N3, 129 and 199 loci were used to estimate the within-host effective population size, respectively. The inferred effective population size for A(H3N2) infections was 284 ± 60 and was 176 ± 41 for A(H1N1)pdm09 infections. Out of 256 loci, 23 (9%) in A(H3N2) specimens and 19/176 (11%) in A(H1N1)pdm09 specimens had positive selection coefficients (Fig. 4b). One A(H3N2) synonymous iSNV (T620C [G197]) was in an HA antigenic site, and 6 A(H1N1)pdm09 and 13 A(H3N2) iSNVs were synonymous. Three of these synonymous A(H1N1)pdm09 iSNVs had corresponding nonsynonymous iSNVs under positive selection. Thirteen A(H3N2) and 10 A(H1N1)pdm09 iSNVs with positive selection coefficients also reached a majority allele frequency. Host age, vaccination status, and antiviral usage did not affect the likelihood of an individual having an iSNV with a positive selection coefficient (Supplementary Table S4).

Global trajectory

We next used the seasonal influenza Nextstrain builds (accessed 31 January 2024) to visualize whether any of the iSNVs in HA and NA that are putatively under positive selection were also identified as increasing in global frequency (Hadfield et al. 2018). Most of the iSNVs identified in our study either were already a dominant allele in the season under evaluation or did not exceed 5% frequency at any time point. However, there were two A(H1N1)pdm09 iSNVs and four A(H3N2) iSNVs that circulated at a significant global frequency after appearing in our cohort (Supplementary Fig. S7). None of these were in antigenic sites. For A(H1N1)pdm09, both iSNVs were from the 2019/20 season; HA_G1628A (A532) is a synonymous iSNV that had a positive selection coefficient. It had a global frequency of ~4% in the 2019/20 season and was fixed in the global population by 2023. HA_A754C (E241A) is a nonsynonymous iSNV that was shared among 19 individuals from 16 households. It was not found at a detectable frequency globally until 2021 and was predominant in 2023. For A(H3N2), HA_T314C (F95) was found in two people during the 2017/18 season and HA_G225A was found in four people during the 2018/19 season. HA_T314C is synonymous and reached a frequency of 3% in 2017. It never became a

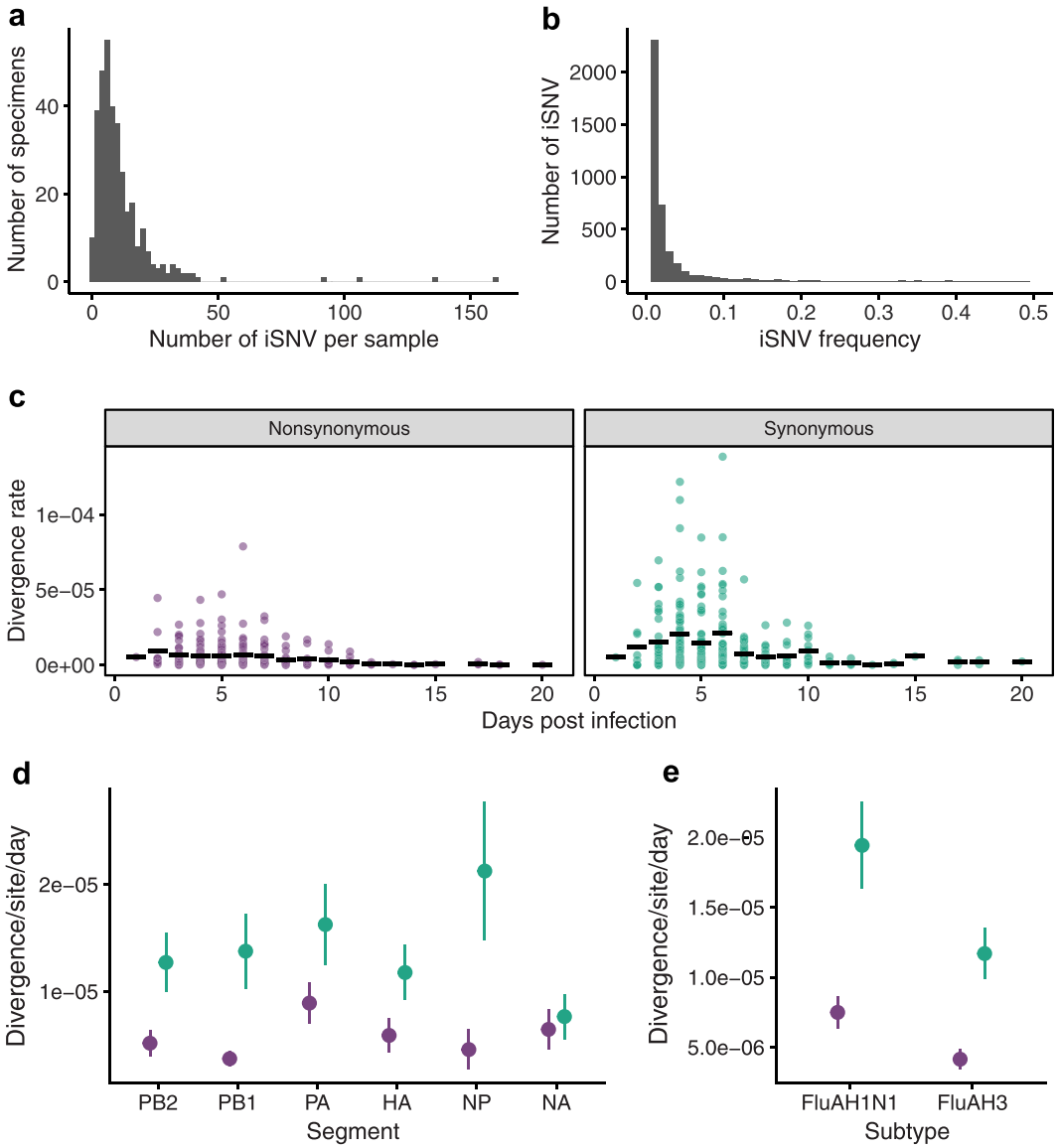

Figure 2. (a) Number of iSNVs per specimen. (b) iSNV frequency. (c) Divergence rate (divergence/site/day) by day postinfection, (d) segment, and (e) subtype (green synonymous, purple nonsynonymous)

dominant allele but did reach a frequency of 10% in 2021. It was previously the dominant allele in 2012 before HA_T314 became dominant. HA_G225A (E66K) is nonsynonymous and was not circulating in 2018. In 2019, it appeared and fluctuated between 0% and 25% until 2022, when it became the dominant allele. It reached 100% in 2024.

HA_C556A (T176K) and HA_G665A (A212) were minor alleles that became major alleles. HA_C556A is a nonsynonymous mutation that was found in the 2017/18 cohort. HA_G665A is a synonymous mutation found in the 2018/19 cohort. A556 fluctuated in frequency as a minor allele in the global population with C556 being the dominant allele, until both were replaced by T starting in 2020. The A allele has fluctuated in global frequency since our sample and has reached a maximum frequency of 20%. The G allele was not circulating at detectable levels when the sample was taken or in the subsequent year. The G was detected in 2023 at a maximum frequency of 2%.

Discussion

In our detailed analysis of serially sampled individuals in a longitudinal household transmission study, we found that within-host IAV populations are highly dynamic and subject to genetic drift and purifying selection. There were differences in divergence rates and the number of iSNVs per sample based on age, and multiple factors influenced iSNV frequencies. However, these differences were minimal and were not reflected in differences in their selection. Positive selection was rare and inconsistently detected with the three methods applied. Our comprehensive evaluation demonstrates that in most cases, the extent of within-host evolution is small and positive selection is only a minor contributor.

Consistent with strong purifying selection, we found low genetic diversity and divergence rates, despite influenza virus's high mutation rate. With the lower frequency threshold, we observed more iSNVs than other studies, but they mainly occurred in the 0.005–0.02 frequency range. Our divergence rates were lower

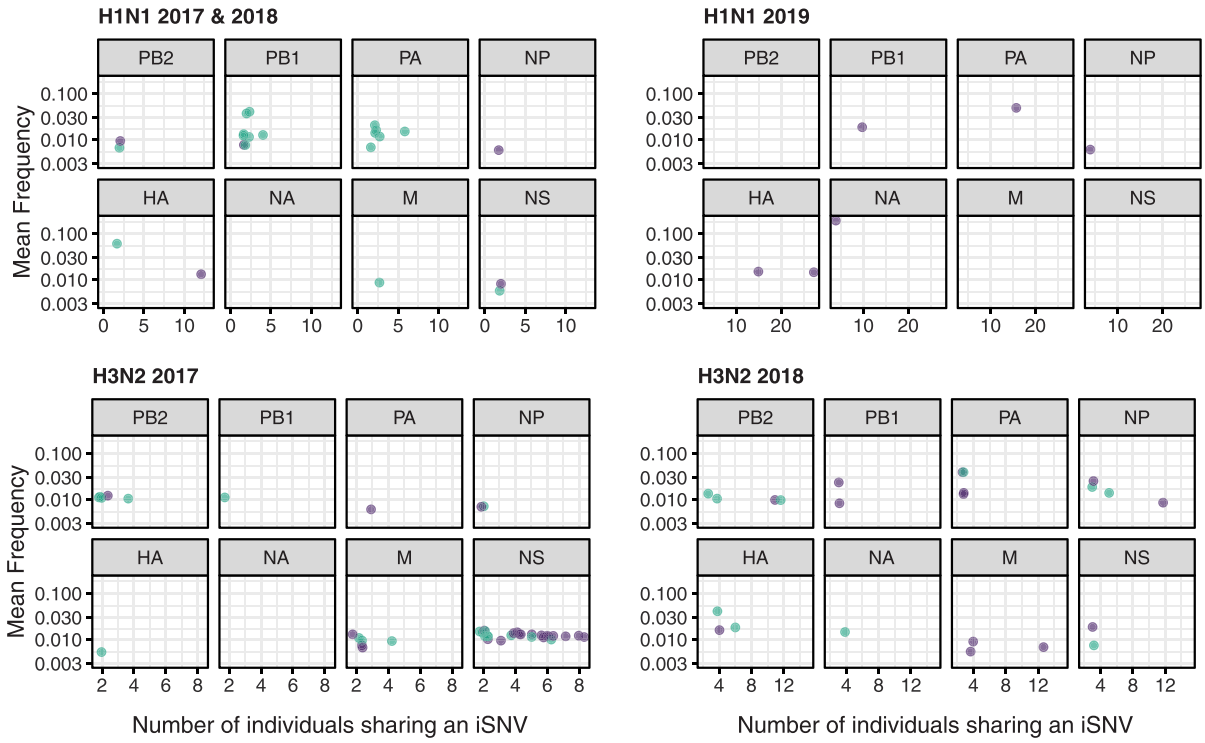

Figure 3. The mean frequency of iSNVs found in multiple individuals from different households after samples with >50 iSNVs were removed. iSNVs from 2017/18 and 2018/19 H1N1 and 2017/18 H3N2 infections are shared in two individuals. iSNVs from 2019/20 H1N1 infections are shared in three individuals, and iSNVs from 2018/19 H3N2 infections are shared in four individuals (green synonymous iSNVs, purple nonsynonymous iSNVs).

than the divergence rates calculated by Xue and Bloom (2020). While the same frequency threshold was used, we applied more rigorous variant calling and potentially had a different distribution of sample timing. Our divergence rates were similar to the rates reported by Han et al. (2021).

By lowering the frequency threshold and using serial sampling, we were able to detect iSNVs that were putatively under selection. However, these iSNVs were mostly outside of HA and NA, and very few were in known antigenic sites. Even when there were selected iSNVs in HA and NA, they rarely achieved a significant frequency in the global population. The small effective population size of within-host populations, which is much smaller than the Ne estimated in chronic infections of immunocompromised hosts (Lumby et al. 2020), reduces the efficiency of selection, and partial immunity may be a relatively weak selective force. If a virus escapes the mucosal membrane to successfully infect a host cell, it takes several days for an antibody-mediated recall response (Morris et al. 2020). The asynchrony of the infection and antibody response would result in minimal selection on antigenic sites within hosts initially. Here, the time between the antibody response and viral clearance may not be sufficient for significant selection. Weak selection combined with a short duration of infection in acutely infected individuals minimizes the evolution of new antigenic variants. We do not deny that new antigenic variants can arise through within-host selection. However, they will be rare events, and newly arising variants, even in antigenic sites, can sweep to fixation due to stochastic dynamics.

Our study focused on typical influenza virus infections from seasonal viruses, but the evolutionary dynamics may differ in atypical situations where positive selection may be prominent. During prolonged infections in some immunocompromised individuals, an antibody-mediated recall response is mounted before the virus is cleared. Here, within-host antigenic selection parallels population-level selection, and mutations that arise within hosts are seen at high frequency globally in subsequent seasons (Xue et al. 2017). Similarly, when positive selection is strong, an acute infection is long enough for adaptive mutations to arise and increase in frequency. Antiviral mutations associated with oseltamivir resistance are routinely seen in acute infections during treatment (Gubareva et al. 2001, Kiso et al. 2004, Koel et al. 2020, Han et al. 2021). Additionally, during the first wave of the 2009 A(H1N1)pdm09 pandemic, there was an overabundance of nonsynonymous mutations within hosts (Han et al. 2021). It is possible that as a new zoonotic spillover, the virus was not already adapted to human hosts allowing for stronger selection within hosts (Han et al. 2021). Based on our prior work and those of others, we suspect that the same principles will generalize to most self-limited respiratory virus infections.

Because our study spanned three influenza seasons and was significantly larger than prior ones, we were able to evaluate the impact of viral and host factors on within-host diversity and evolutionary rate. Consistent with the observed differences in shedding, we observed differences in the levels of genetic diversity across age groups. Children had faster rates of evolution and a greater number of iSNVs per specimen compared to adolescents, while adolescents had higher iSNV frequencies than adults or children. Although these comparisons achieved statistical significance, they are unlikely to be biologically meaningful. The differences between ages are very small and had minimal impact on our tests for selection. In our cohort, positively selected iSNVs were equally likely to have been identified in

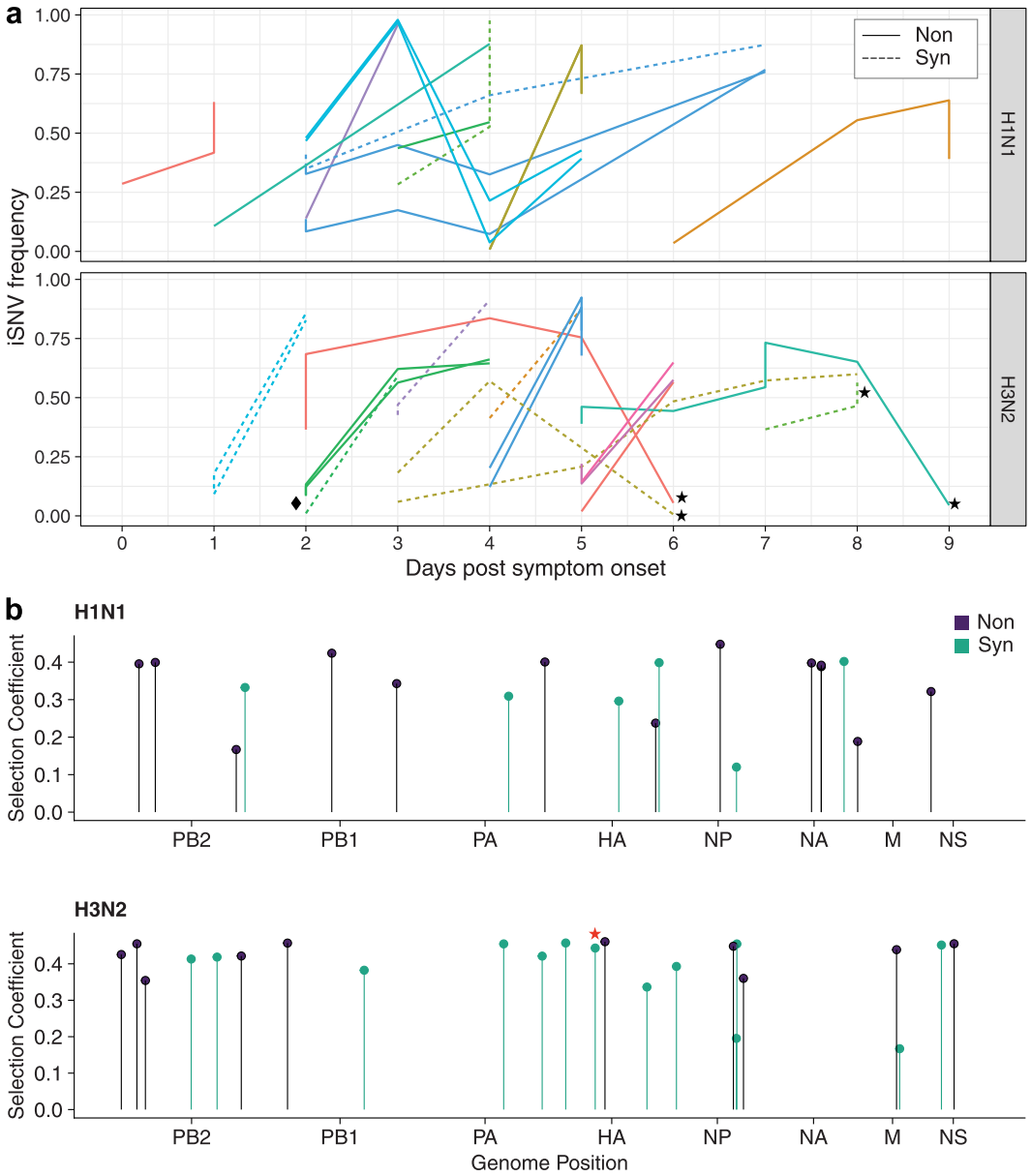

Figure 4. (a) Allele trajectories of iSNVs that go from minor to major allele over the course of an infection. Lines are colored by individual. Dashed lines are synonymous iSNVs and solid lines are nonsynonymous iSNVs. The household symptom onset date was used for individuals with asymptomatic infections. Green lines next to the diamond (♦) are from Individual 1 811 602. (b) WFABC selection coefficients for iSNVs under positive selection. Stars indicate iSNVs in HA antigenic sites in both (a) and (b).

children, adolescents, or adults; children were less likely to contribute to shared iSNVs than adults. Although children and adolescents may play an outsized role in influenza epidemics due to increased shedding and their social networks (Worby et al. 2015), their within-host dynamics are remarkably similar to those of adults.

Our study has multiple strengths. The participants were from the community and were representative of the general population, making the results widely applicable. Due to the diversity in our cohort, we were able to study the effects of age, vaccination status, and antiviral usage. We also used multiple methods to detect positive selection. Allele trajectory methods are more effective, but identifying shared variants allowed us to test for positive selection when there was only a single specimen. Additionally, we applied stringent variant calling criteria that were benchmarked to ensure high confidence in variant calls.

There are several limitations to our study. We used only nasal swabs and would potentially miss selected sites if there was compartmentalization. However, nasal swabs likely sample the most relevant population for transmission, as virions replicating in the soft palate or nasal epithelial cells form the population that is most likely to be transmitted (Varble et al. 2014, Lakdawala et al. 2015, Richard et al. 2020). In ferrets, compartmentalization in the lungs occurs through a series of bottlenecks (Amato et al. 2022). This leads to significant genetic drift, which further masks any signals of positive selection. Therefore, it is unlikely that a more comprehensive sampling of the respiratory tract would change our results. Despite our best attempts to mitigate

it, there is always the possibility of sequencing errors and false iSNV calls.

Our work was only in a US cohort, and there is the possibility that the results will not generalize to other settings. However, the viruses circulating in our cohort were representative of seasonal influenza viruses globally (Hammond et al. 2018, 2019, Karlsson et al. 2021), and many cases were not medically attended. Additionally, in 2020, the widespread mitigation measures in response to the coronavirus disease 2019 pandemic severely curtailed IAV circulation (Dhanasekaran et al. 2022). IAV reappeared in 2021 after an intense bottleneck. In contrast to typical patterns, stochastic processes dominated globally, complicating our ability to connect within-host processes to global outcomes. However, our results are similar to other acute seasons and all A(H3N2) specimens were collected one to two seasons prior to the severe acute respiratory syndrome virus 2 (SARS-CoV-2) outbreak.

Despite multiple studies with varying populations and approaches, clear evidence of within-host antigenic drift in acute infections is lacking. Given the rigor of our methods and the data from other studies, we find that acute influenza virus infections are dominated by stochastic forces (mutation and drift) with little evidence for positive selection regardless of age, vaccination status, antiviral use, or subtype. This calls into question whether this is useful as a surveillance strategy. While positively selected variants exist, a large number of people would need to be closely followed to find them. However, our characterization of divergence rates within hosts and the impact of viral and host factors are important for understanding and modeling how within-host processes feed into larger evolutionary dynamics. Other RNA respiratory viruses, such as influenza B (Valesano et al. 2020), SARS-CoV-2 (Braun et al. 2021, Lythgoe et al. 2021, Hannon et al. 2022, Bendall et al. 2023, Farjo et al. 2024), and respiratory syncytial virus (Lin et al. 2021), have low within-host genetic diversity and similar infection dynamics to IAV. The phenomenon of strong immune selection at the population level and stochastic processes dominating within hosts may be widespread in acute respiratory infections.

Author contributions

A.S.L., C.G.G., and H.K.T. were involved in conceptualization. All authors were involved in data curation. E.E.B., Y.Z., and A.S.L. were involved in formal analysis. A.S.L., E.T.M., C.G.G., and H.K.T. were involved in funding acquisition. All authors were involved in investigation. All authors were involved in methodology. A.S.L., C.G.G., and H.K.T. were involved in project administration. All authors were involved in resources.

Supplementary data

Supplementary data is available at *VEVOLU Journal* online.

Conflict of interest: All authors have completed International Committee of Medical Journal Editors disclosure forms (www.icmje.org/coi_disclosure.pdf). C.G.G. reports grants from the National Institutes of Health (NIH), Centers for Disease Control and Prevention (CDC), Agency for Healthcare Research and Quality, Food and Drug Administration, and Campbell Alliance/Syneos Health; consulting fees; and participation on a data safety and monitoring board for Merck, outside the submitted work. N.H. reports grants from Sanofi, Quidel, and Merck, outside the submitted work. A.S.L. reports receiving grants from CDC, NIH, Burroughs Wellcome Fund, and Flu Lab and consulting fees from Roche, outside the submitted work. E.T.M. reports receiving a grant from Merck, outside the submitted work. The findings and conclusions in this report are those of the authors and do not necessarily represent the official position of the CDC.

Funding

Primary funding for the FluTES study was provided by the US CDC (5U01IP001083). C.G.G. was partially supported by NIH K24A I148459. Scientists from the US CDC participated in all aspects of this study, including its design, analysis, interpretation of data, writing the report, and the decision to submit the article for publication. Sequencing and associated analysis were supported by a Burroughs Wellcome Fund Investigator in the Pathogenesis of Infectious Diseases Award (to A.S.L.), NIH R01 AI148371 (to A.S.L. and E.T.M.), and the Penn Center for Excellence in Influenza Research and Response, Penn-CEIRR, NIH 75N93021C00015 (to A.S.L. and E.T.M.).

Data availability

Raw sequence data are available at the NCBI Sequence Read Archive (SRA) under BioProject PRJNA1085292. The analysis code is available at https://github.com/lauringlab/Flutes_within-host_evolution.

References

Amato KA, Haddock LA, Braun KM *et al.* Influenza A virus undergoes compartmentalized replication in vivo dominated by stochastic bottlenecks. *Nat Commun* 2022;**13**:3416.

Baccam P, Beauchemin C, Macken CA *et al.* Kinetics of influenza A virus infection in humans. *J Virol* 2006;**80**:7590–99.

Beauchemin CAA, Handel A. A review of mathematical models of influenza A infections within a host or cell culture: lessons learned and challenges ahead. *BMC Public Health* 2011;**11 Suppl 1**:S7.

Bedford T, Riley S, Barr IG *et al.* Global circulation patterns of seasonal influenza viruses vary with antigenic drift. *Nature* 2015;**523**:217–20.

Bendall EE, Callear AP, Getz A *et al.* Rapid transmission and tight bottlenecks constrain the evolution of highly transmissible SARS-CoV-2 variants. *Nat Commun* 2023;**14**:272.

Bodewes R, de Mutsert G, van der Klis FRM *et al.* Prevalence of antibodies against seasonal influenza A and B viruses in children in Netherlands. *Clin Vaccine Immunol* 2011;**18**:469–76.

Braun KM, Moreno GK, Wagner C *et al.* Acute SARS-CoV-2 infections harbor limited within-host diversity and transmit via tight transmission bottlenecks. *PLoS Pathog* 2021;**17**:e1009849.

Carrat F, Vergu E, Ferguson NM *et al.* Time lines of infection and disease in human influenza: a review of volunteer challenge studies. *Am J Epidemiol* 2008;**167**:775–85.

Dawood FS, Chung JR, Kim SS *et al.* Interim estimates of 2019–20 seasonal influenza vaccine effectiveness—United States, February 2020. *MMWR Morb Mortal Wkly Rep* 2020;**69**:177–82.

De P, Farley A, Lindson N *et al.* Systematic review and meta-analysis: influence of smoking cessation on incidence of pneumonia in HIV. *BMC Med* 2013;**11**:15.

Debbink K, McCrone JT, Petrie JG *et al.* Vaccination has minimal impact on the intrahost diversity of H3N2 influenza viruses. *PLoS Pathog* 2017;**13**:e1006194.

Dhanasekaran V, Sullivan S, Edwards KM *et al.* Human seasonal influenza under COVID-19 and the potential consequences of influenza lineage elimination. *Nat Commun* 2022;**13**:1721.

Dinis JM, Florek KR, Fatola OO *et al*. Deep sequencing reveals potential antigenic variants at low frequencies in influenza A virus-infected humans. *J Virol* 2016;**90**:3355–65.

Doud MB, Hensley SE, Bloom JD. Complete mapping of viral escape from neutralizing antibodies. *PLoS Pathog* 2017;**13**:e1006271.

Farjo M, Koelle K, Martin MA *et al*. Within-host evolutionary dynamics and tissue compartmentalization during acute SARS-CoV-2 infection. *J Virol* 2024;**98**:e0161823.

Foll M, Shim H, Jensen JD. WFABC: a Wright-Fisher ABC-based approach for inferring effective population sizes and selection coefficients from time-sampled data. *Mol Ecol Resour* 2015;**15**:87–98.

Garten R, Blanton L, Elal AIA *et al*. Update: influenza activity in the United States during the 2017–18 season and composition of the 2018–19 influenza vaccine. *MMWR Morb Mortal Wkly Rep* 2018;**67**:634–42.

Grubaugh ND, Gangavarapu K, Quick J *et al*. An amplicon-based sequencing framework for accurately measuring intrahost virus diversity using PrimalSeq and iVar. *Genome Biol* 2019;**20**:8.

Gubareva LV, Kaiser L, Matrosovich MN *et al*. Selection of influenza virus mutants in experimentally infected volunteers treated with oseltamivir. *J Infect Dis* 2001;**183**:523–31.

Hadfield J, Megill C, Bell SM *et al*. Nextstrain: real-time tracking of pathogen evolution. *Bioinforma Oxf Engl* 2018;**34**:4121–23.

Hammond A, Hundal K, Laurenson-Schafer H *et al*. Review of the 2018–2019 influenza season in the northern hemisphere. *Wkly Epidemiol Rec* 2019;**94**:345–63.

Hammond A, Laurenson-Schafer H, Marsland M *et al*. Review of the 2017–2018 influenza season in the northern hemisphere. *Wkly Epidemiol Rec* 2018;**93**:429–44.

Han AX, Felix Garza ZC, Welkers MR *et al*. Within-host evolutionary dynamics of seasonal and pandemic human influenza A viruses in young children. *eLife* 2021;**10**:e68917.

Hannon WW, Roychoudhury P, Xie H *et al*. Narrow transmission bottlenecks and limited within-host viral diversity during a SARS-CoV-2 outbreak on a fishing boat. *Virus Evol* 2022;**8**:1–9.

Hoffmann E, Stech J, Guan Y *et al*. Universal primer set for the full-length amplification of all influenza A viruses. *Arch Virol* 2001;**146**:2275–89.

Karlsson EA, Mook PA, Vandemaele K *et al*. Review of global influenza circulation, late 2019 to 2020, and the impact of the COVID-19 pandemic on influenza circulation. *Wkly Epidemiol Rec* 2021;**25**:241–64.

Kilbourne ED, Smith C, Brett I *et al*. The total influenza vaccine failure of 1947 revisited: major intrasubtypic antigenic change can explain failure of vaccine in a post-World War II epidemic. *Proc Natl Acad Sci USA* 2002;**99**:10748–52.

Kiso M, Mitamura K, Sakai-Tagawa Y *et al*. Resistant influenza A viruses in children treated with oseltamivir: descriptive study. *Lancet Lond Engl* 2004;**364**:759–65.

Koel BF, Vigeveno RM, Pater M *et al*. Longitudinal sampling is required to maximize detection of intrahost A/H3N2 virus variants. *Virus Evol* 2020;**6**:veaa088.

Lakdawala SS, Jayaraman A, Halpin RA *et al*. The soft palate is an important site of adaptation for transmissible influenza viruses. *Nature* 2015;**526**:122–25.

Langmead B, Salzberg SL. Fast gapped-read alignment with Bowtie 2. *Nat Methods* 2012;**9**:357–59.

Lin G-L, Drysdale SB, Snape MD *et al*. Distinct patterns of within-host virus populations between two subgroups of human respiratory syncytial virus. *Nat Commun* 2021;**12**:5125.

Lumby CK, Zhao L, Breuer J *et al*. A large effective population size for established within-host influenza virus infection. *eLife* 2020;**9**:e56915.

Luo S, Reed M, Mattingly JC *et al*. The impact of host immune status on the within-host and population dynamics of antigenic immune escape. *J R Soc Interface* 2012;**9**:2603–13.

Lythgoe KA, Hall M, Ferretti L *et al*. SARS-CoV-2 within-host diversity and transmission. *Science* 2021;**372**:eabg0821.

McCrone JT, Lauring AS, Dermody TS. Measurements of intrahost viral diversity are extremely sensitive to systematic errors in variant calling. *J Virol* 2016;**90**:6884–95.

McCrone JT, Woods RJ, Martin ET *et al*. Stochastic processes constrain the within and between host evolution of influenza virus. *eLife* 2018;**7**:e35962.

Morris DH, Petrova VN, Rossine FW *et al*. Asynchrony between virus diversity and antibody selection limits influenza virus evolution. *eLife* 2020;**9**:e62105.

Ng S, Lopez R, Kuan G *et al*. The timeline of influenza virus shedding in children and adults in a household transmission study of influenza in Managua, Nicaragua. *Pediatr Infect Dis J* 2016;**35**:583–86.

Picard Toolkit. Broad Inst. GitHub Repository. 2019.

Richard M, van den Brand JMA, Bestebroer TM *et al*. Influenza A viruses are transmitted via the air from the nasal respiratory epithelium of ferrets. *Nat Commun* 2020;**11**:766.

Rolfes MA, Talbot HK, McLean HQ *et al*. Household transmission of influenza A viruses in 2021–2022. *JAMA* 2023;**329**:482–89.

Salk JE, Suriano PC. Importance of antigenic composition of influenza virus vaccine in protecting against the natural disease; observations during the winter of 1947–1948. *Am J Public Health Nations Health* 1949;**39**:345–55.

Smith BJ. boa: An R package for MCMC output convergence assessment and posterior inference. *J Stat Softw* 2007;**21**:1–37.

Smith DJ, Lapedes AS, de Jong JC *et al*. Mapping the antigenic and genetic evolution of influenza virus. *Science* 2004;**305**:371–76.

Sobel Leonard A, McClain MT, Smith GJD *et al*. Deep sequencing of influenza A virus from a human challenge study reveals a selective bottleneck and only limited intrahost genetic diversification. *J Virol* 2016;**90**:11247–58.

Sobel Leonard A, McClain MT, Smith GJD *et al*. The effective rate of influenza reassortment is limited during human infection. *PLoS Pathog* 2017a;**13**:e1006203.

Sobel Leonard A, Weissman DB, Greenbaum B *et al*. Transmission bottleneck size estimation from pathogen deep-sequencing data, with an application to human influenza A virus. *J Virol* 2017b;**91**:e00171–17.

Valesano AL, Fitzsimmons WJ, McCrone JT *et al*. Influenza B viruses exhibit lower within-host diversity than influenza A viruses in human hosts. *J Virol* 2020;**94**:e01710–19.

Varble A, Albrecht R, Backes S *et al*. Influenza A virus transmission bottlenecks are defined by infection route and recipient host. *Cell Host Microbe* 2014;**16**:691–700.

Visher E, Whitefield SE, McCrone JT *et al*. The mutational robustness of influenza A virus. *PLoS Pathog* 2016;**12**:e1005856.

Volkov I, Pepin KM, Lloyd-Smith JO *et al*. Synthesizing within-host and population-level selective pressures on viral populations: the impact of adaptive immunity on viral immune escape. *J R Soc Interface* 2010;**7**:1311–18.

Worby CJ, Chaves SS, Wallinga J *et al*. On the relative role of different age groups in influenza epidemics. *Epidemics* 2015;**13**:10–16.

Xu X, Blanton L, Elal AIA *et al*. Update: influenza activity in the United States during the 2018–19 season and composition of the 2019–20 influenza vaccine. *MMWR Morb Mortal Wkly Rep* 2019;**68**:544–51.

Xue KS, Bloom JD. Linking influenza virus evolution within and between human hosts. *Virus Evol* 2020;**6**:veaa010.

Xue KS, Stevens-Ayers T, Campbell AP *et al*. Parallel evolution of influenza across multiple spatiotemporal scales. *eLife* 2017;**6**:e26875.

Virus Evolution, 2024, 10(1), veae084 , DOI: https://doi.org/10.1093/ve/veae084, Advance Access Publication 3 October 2024, Research Article